

Influence of temperature on shock compressibility and spall strength of ABS under weak shock waves

© I.A. Cherepanov, A.S. Savinykh, G.V. Garkushin, S.V. Razorenov

Federal Research Center for Problems of Chemical Physics and Medical Chemistry, Russian Academy of Sciences, 142432 Chernogolovka, Moscow region, Russia
email: i.cherepanov95@yandex.ru

Received September 26, 2023

Revised November 2, 2023

Accepted November 10, 2023

The influence of temperature on the strength characteristics of ABS (copolymer of acrylonitrile, butadiene and styrene) under high strain rate is investigated. Spall strength was measured at a maximum compression stress of 0.6 GPa in the initial temperature range of samples 20–115°C. An explanation is proposed for the abnormal increase in the value of the spall strength when the glass transition temperature is exceeded based on the analysis of a possible change in the internal structure. The dependences of the shock wave velocity on the particle velocity (Hugoniot) in the range of maximum shock compression stresses from 0.1 GPa to 1.0 GPa at different temperatures are constructed.

Keywords: ABS, shock waves, deformation, temperature, spall strength, Hugoniot.

DOI: 10.61011/JTF.2024.01.56910.247-23

Introduction

ABS is a copolymer of three monomers such as acrylonitrile, butadiene and styrene and nowadays it is one of the most promising structural polymer materials. The active use of ABS as a product for 3D printing, together with its mechanical properties, suggests its widespread use in various sectors of industry. The question of the ABS properties at high strain rates over a wide temperature range remains relevant in view of the possible use of ABS products, including their use under elevated temperatures and pulse loads. This is primarily attributable to the fact that most theoretical and mathematical models describing the failure of polymer materials at high strain rates usually rely on data mainly obtained from experiments with polycarbonate or polymethylmethacrylate [1–5].

The resistance of ABS to tensile stresses under quasi-static loading conditions was studied in [6,7]. It was noted that the yield strength, Young's modulus and the rate of strain hardening increase at room temperature with the increase of the strain rate, and a phenomenological model was proposed describing the deformation behavior of ABS under dynamic tensile stresses. A similarity between the experimental data obtained for the source material and for samples subjected to the 3D-printing procedure was noted in [7].

The influence of temperature and compression strain rate on the nature of the ABS failure in the range of strain rates 1000–4000 s⁻¹ is studied in [8]. It was shown that the strain rate decreases with the increase of the temperature because of the softening of the material, and a direct relationship between the strain rate and the applied load was also noted. An increase of the strain rate up to of 4000 s⁻¹ results in a complete destruction of the samples.

A special attention should be paid to the influence of temperature and the transition from a crystalline state to a vitreous state one on the strength properties of ABS. Therefore, the dependence of mechanical properties on the strain rate at temperatures below the glass transition point was shown in [9], which well describes the behavior of the material within the time approach, as it occurs in metals. The paper also describes in detail the nature of the failure and analyzes the nature of the nucleation and propagation of cracks in the material.

The resistance to tensile stresses under shock loads in a wide temperature range, including the glass transition point, was studied on the basis of polymethylmethacrylate and polycarbonate in [10,11]. It was shown that the value of the spall strength significantly decreases and the values of the bulk speed of sound also decrease when the glass transition temperature is exceeded, while the slope of the Hugoniot practically does not change.

Studies of polymer materials in the temperature range, including the glass transition temperature of polymers, have been started only recently. The analysis of experimental data is complicated, in particular, by the lack of information on bulk compressibility in the range of low and moderate pressures [12]. The purpose of this work is to study the effect of temperature on the shock compressibility and strength of ABS in the temperature range from 20 to 115°C, including its transition to a vitreous state.

1. Material and test setup

The experiments were carried out with samples of ABS of grade 2332 produced by SIBUR with a thickness of 2 ± 0.1 mm and 4 ± 0.1 mm, with a diameter of 30 mm, cut from a single sheet of the appropriate thickness. The

initial temperature of the samples ranged from 20 to 115°C. The differential scanning calorimetry method [13] was used to determine the glass transition temperature of T_g ABS and it was found that the glass transition temperature is $T_g = 105^\circ\text{C}$. The density of ABS measured by hydrostatic weighing was $\rho_0 = 1.040\text{ g/cm}^3$, the measured longitudinal speed of sound was $c_l = 2.199\text{ km/s}$.

A pneumatic gun with a diameter of 50 mm was used for the shock wave loading of the studied samples. The receiving chamber and the pneumatic barrel were evacuated before the experiments. The spall strength was measured during loading of 2 mm thick samples by 1 mm thick aluminum impactors accelerated to 250 m/s. The scheme of experiments to determine the spall strength of ABS is shown in Fig. 1, *a*. The maximum compression stress in ABS was 0.58 GPa in this setup. Moreover, experiments were conducted at room temperature to measure the spall strength of ABS loaded by 2 and 0.9 mm thick aluminum impactors accelerated to 360 and 190 m/s, which corresponds to maximum compression stresses of 0.86 and 0.43 GPa.

A second series of experiments was performed to construct the dependence of the velocity of the shock wave U_s on the particle velocity u_p Hugoniot. The loading setup is shown in Fig. 1, *b*. 7 mm thick aluminum impactor accelerated to $210 \pm 10\text{ m/s}$ or $260 \pm 10\text{ m/s}$ was used for shock wave loading. The sample was loaded through 5 mm thick aluminum base plate on which the 4 mm thick test sample with an unknown Hugoniot and 1.2 mm thick soda-lime glass were placed. The principle of this method is that multiple reverberation of waves occurs in the glass plate—witness after the shock wave passes through the sample. The maximum compression stresses (σ_{max}) were 0.82 or 1.02 GPa, respectively, at the first rereflection of the wave in soda-lime glass which is significantly lower than the Hugoniot elastic limit (σ_{HEL}) of this glass. The values (σ_{HEL}) for soda-lime glass range from 3.5 to 7 GPa according to [14], i.e. the reverberation of waves in soda-lime glass occurs in the elastic region in these experiments. The glass thickness used at a higher value of the speed of sound ($c_l = 5.720\text{ km/s}$ in glass) allows for obtaining several rereflections of waves in glass without interaction with the compression wave reflected from the base plate. This formulation makes it possible to determine multiple points on the Hugoniot at a time in one experiment.

The velocity of the free surface of the samples was recorded using the VISAR laser Doppler velocimeter [15] as a function of time $u_{fs}(t)$ with a resolution of $\sim 1\text{ ns}$ in all experiments. The laser radiation was reflected from 7 μm thick aluminum foil glued to the sample using a two-component epoxy adhesive, the operating temperature range of which includes the temperatures of the samples achieved in experiments. The samples were heated by ceramic heater with a nichrome spiral, which was placed either at the back surface of the sample (Fig. 1, *a*),

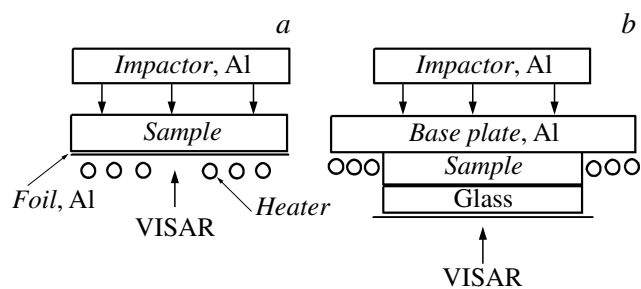


Figure 1. Setup of experiments for impact loading and recording of free surface velocity profiles of ABS samples at room and elevated temperatures. *a* — measurement of spall strength, *b* — measuring the dependence $U_s - u_p$.

or was placed on an aluminum base plate (Fig. 1, *b*). The temperature was controlled by two chromel-alumel thermocouples. One thermocouple was glued from the end of the sample, the other thermocouple was glued into the sample at a distance of $\sim 6-7\text{ mm}$ from the place of recording of the velocity of the free surface in the case of determination of the spall strength or into the glass–sample contact point in a series of experiments for measuring the dependence $U_s - u_p$. The difference between the thermocouple readings was not greater than 2–3°C. The use of two thermocouples ensured a definitive control of the glass transition process. The average sample heating rate was $\sim 0.05^\circ\text{C/s}$.

2. Measurement results

Fig. 2 shows the free surface velocity profiles of 2 mm thick ABS samples loaded by 0.9, 1 and 2 mm thick aluminum impactors with the velocities of 190, 250 and 360 m/s, respectively, recorded at room temperature. The maximum compression stresses reached in these experiments were 0.43, 0.58 and 0.86 GPa. There are no signs of elastic strain on the profiles in the form of an exposure of elastic precursor on the free surface. Only the exposure of compression wave on the free surface is recorded. The appearance of a part of the rarefaction wave preceding the spall fracturing is recorded after the maximum surface velocity is reached. The spall pulse is not registered on the surface profiles. An increase of the maximum compression stress results in an increase of the shock rarefaction of the shock wave and, accordingly, the rarefaction wave, which results in a reduction of the time needed for the spall fracture moment to reach the free surface (dashed line).

Fig. 3 shows the free surface velocity profiles of 2 mm thick ABS samples loaded by 1 mm thick aluminum impactor accelerated to 250 m/s recorded in the initial temperature range from 20 to 115°C. The free surface velocity slightly changes with an increase of the temperature slightly decreasing when the glass transition temperature is exceeded. The time of appearance of the spall pulse to the surface, marked with arrows, is the same in all experiments.

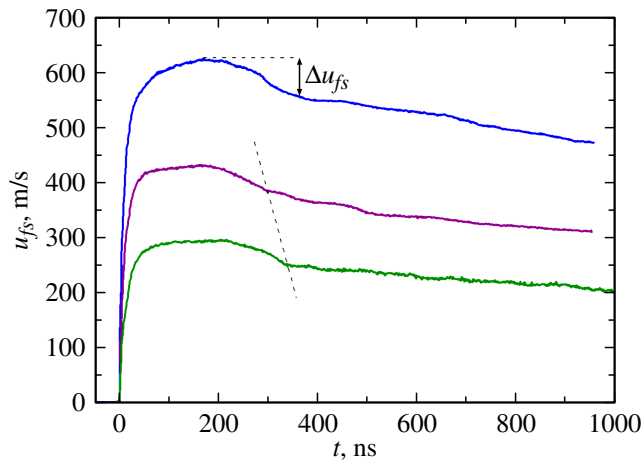


Figure 2. The free surface velocity profiles of 2 mm thick ABS samples at 20°C loaded by 0.9, 1 and 2 mm thick aluminum impactors with velocities of 190, 250 and 360 m/s, respectively.

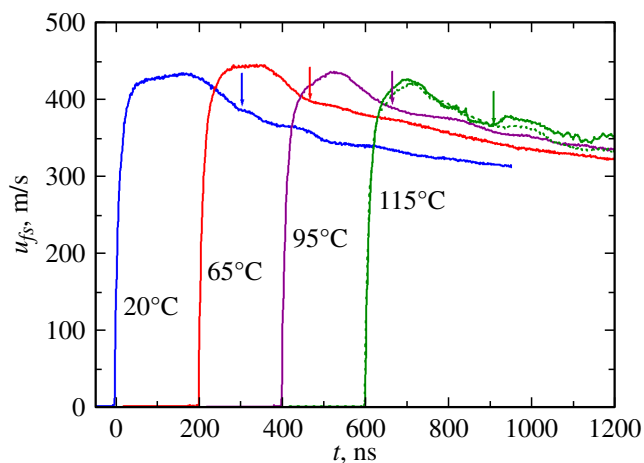


Figure 3. Free surface velocity profiles of ABS samples loaded by 1 mm thick aluminum impactor at a velocity of 250 m/s in the temperature range from 20 to 115°C. The arrows indicate the time points of the spall fracture.

The wave profiles show that the nature of the spall fracture of ABS at temperatures below the glass transition temperature (20, 60 and 95°C) is more similar to the dynamic destruction in elastomers [16] than in thermos, such as polymethylmethacrylate and polycarbonate [10,11]. The spall pulse is not recorded during tensile after the part of the rarefaction wave reaches the surface. The detaching surface layer decelerates for a prolonged period retaining its bond with the main part of the sample. Thus, the spall strength measured value can characterize the conditions of the nucleation of micro-gaps, but not the conditions of complete rupture like in the rubber. The prolonged decrease of the free surface velocity after the spall pulse reaches it is determined by the tensile resistance of the ABS.

The spall pulse becomes more pronounced at 115°C. It is possible to assume based on the data from [9] that

this phenomenon may be explained by the mechanisms of destruction of the material. The authors note that the material begins to homogenize when the temperature reaches 100°C unlike low-temperature experiments, where the lamination resulting from the sample manufacturing method is clearly expressed.

The spall strength of ABS was determined using $\sigma_{sp} = 1/2\rho_0c_b(\Delta u_{fs} + \delta)$ ratio [17,18], where ρ_0 — initial density, c_b — bulk sound velocity, δ — correction for the distortion of the velocity profile because of the difference of the velocities of the elastic front of the spall pulse and the velocity of the part of the incident unloading wave in front of it. The correction value δ was assumed to be zero for calculation of the spall strength since ABS does not exhibit any elastic properties during impact compression. Δu_{fs} — velocity decrement, the difference between the maximum value of the free surface velocity and the minimum velocity in the unloading wave (Fig. 2). The dependence of the density of ABS on the initial temperature was taken from [19]. Fig. 4 shows the free surface velocity decrements taken from the free surface velocity profiles shown in Fig. 2 and 3. An increase of the intensity of impact compression results in an increase of Δu_{fs} in the studied pressure range at room temperature which is not the case with polycarbonate [11]. The velocity decrement slightly decreases when the temperature of the samples increases to the glass transition temperature and it sharply increases after the completion of the glass transition process.

The bulk speeds of sound were determined in the second series of experiments with elastic wave reverberation in soda-lime glass using a thick sample of ABS (Fig. 1, b). Fig. 5 shows the measured free surface velocity profiles of the witness glass plate loaded by 7 mm thick aluminum impactor accelerated to 210 and 260 m/s in the initial temperature range of 20–115°C. Velocity steps are recorded on the free surface velocity profiles which are caused by the repeated rereflection of the elastic wave in the form of compression waves in case of reflection from

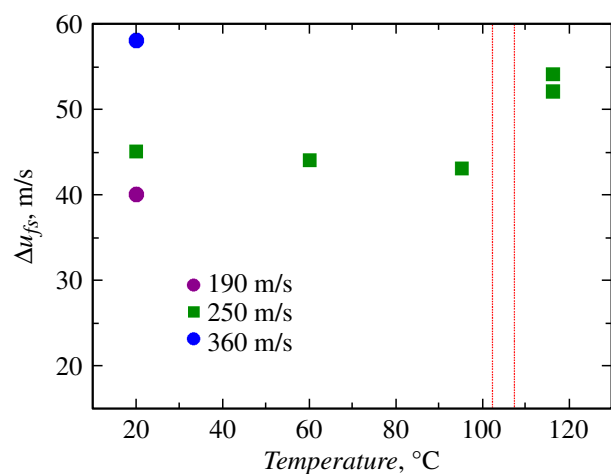


Figure 4. Dependence of the decrement of the ABS velocity on temperature at different impact velocities. The temperatures of the beginning and end of glass transition are shown by dotted lines.

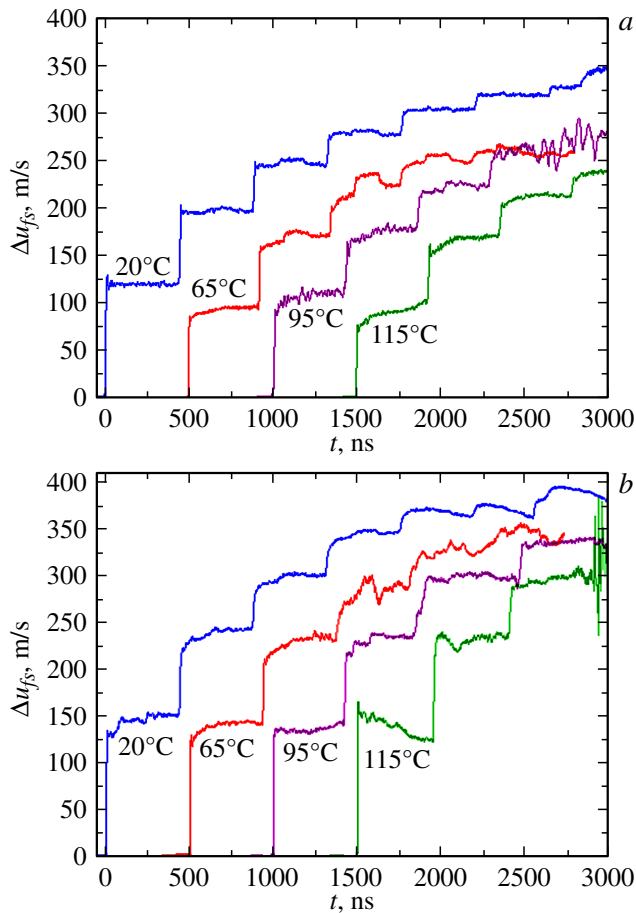


Figure 5. Free surface velocity profiles of soda-lime glass samples loaded by 7 mm thick aluminum impactor accelerated to 210 (a) and 260 m/s (b) in the temperature range of 20–115°C.

ABS with lower dynamic compressibility, and in the form of rarefaction waves in case of reflection from the glass free surface. The first 2–4 steps in each experiment were taken characterized by a smooth front and the absence of significant oscillations for the analysis of the obtained results. The free surface velocity slightly decreases as the temperature continues to increase after the appearance of the first and subsequent compression waves. The time of appearance of re-reflected elastic waves to the free surface is determined by the thickness of the glass plate and the thickness of the foil. The results of measurements demonstrate with good accuracy the equality of times for each stage in each experiment. The ratio of the thickness of the glass plate, taking into account the glued foil, to the time difference between the appearances to the free surface of the steps determines the measured value of the longitudinal speed of sound of soda-lime glass with a good accuracy.

Fig. 6 shows an example of the restored values of pressure and particle velocity at each „step“ during the reverberation of a wave in the glass of one of the free surface velocity profiles shown in Fig. 5. Both materials acquire the same particle velocity and pressure when the

shock wave appearances the ABS into the glass. The corresponding point on the $P-u$ diagram is defined as the intersection of the glass Hugoniot constructed using the value of the free surface velocity equal to zero, and the unloading isentropy constructed using the value of the free surface velocity equal to the free surface velocity at the first step. The specular reflected Hugoniot in the area of elastic strain of glass relative to the intersection point should completely coincide with the unloading isentropy. The algorithm for determination of further points of equality of pressures and particle velocities after the next reflection of the rarefaction wave from ABS in the form of a compression wave is similar to the determination of the first equality point. However, the Hugoniot of the glass exists the point with the value of free surface velocity of the previous stage, and the Hugoniot describing the unloading wave from the point with the value of the free surface velocity of the next stage. Each such point at the ABS–glass boundary is marked with a red square in Fig. 6. The points in Fig. 6, marked with a red star, are the desired values of pressure–particle velocity for ABS, obtained using a specular reflection relative to the intersection with the aluminum deceleration adiabat, which coincides with the value of the impactor velocity. A similar experimental setup for the determination of Hugoniot in polyurea was proposed in [20]. Parameters of changes of the sound speed and density of soda-lime glass depending on temperature are taken from [21–23]. The dependence U_S-u_p was determined from the dependencies $P-u_p$ obtained for ABS using the ratio $P = \rho_0 \cdot U_S \cdot u_p$.

The obtained dependences U_S-u_p for ABS in the studied temperature range are shown in Fig. 7. The value of the bulk speed of sound c_b for calculation of the spall strength was assumed to be equal to c_0 depending on the velocity of the shock wave U_S on the particle velocity u_p , $U_S = c_0 + bu_p$, where the coefficient b is determined by the slope of the linear dependence. The obtained dependences U_S-u_p lie lower with an increase of temperature than the Hugoniot at a lower temperature,

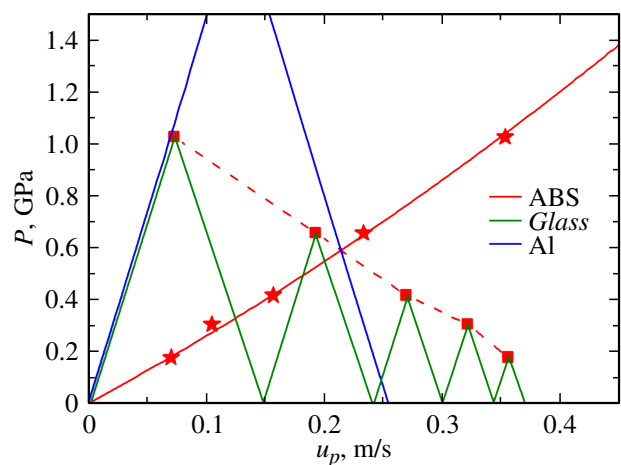


Figure 6. $P-u_p$ diagram of shock wave interactions in Hugoniot measurement experiments.

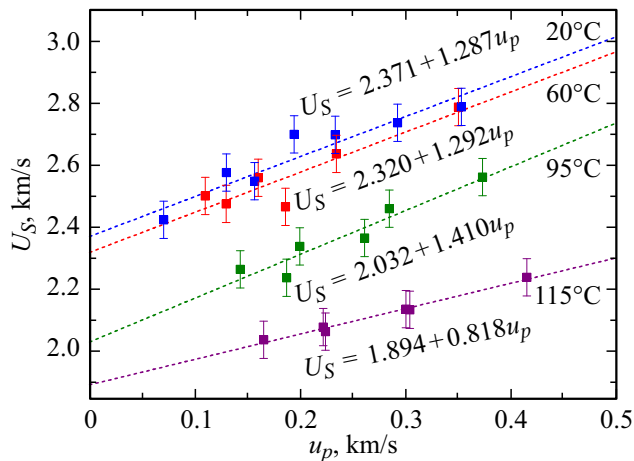


Figure 7. The results of measurements of the Hugoniot of the ABS in the temperature range of 20–115°C.

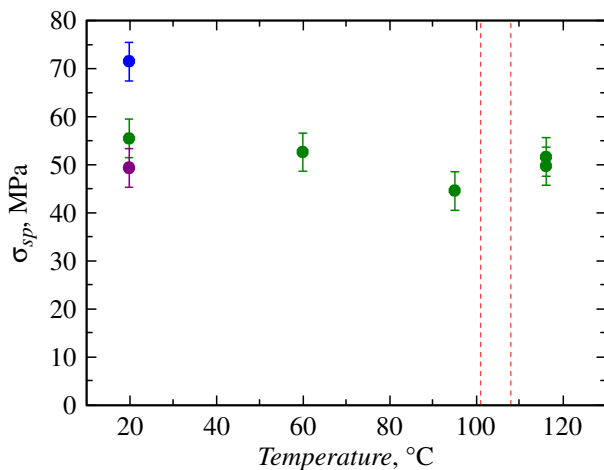


Figure 8. The dependence of the ABS spall strength on the initial temperature; dotted lines show the temperatures of the beginning and end of glass transition.

as a result the bulk speed of sound decreases with an increase of the temperature. The slope of the Hugoniots, characterized by a coefficient of b , remains approximately the same up to the glass transition temperature; this value significantly decreases when the glass transition temperature is exceeded. It should be noted that the measured value of the longitudinal speed of sound in ABS that is equal to 2.199 km/s at room temperature is significantly lower than $c_0 = 2.371$ km/s, therefore, the appearance of the elastic precursor to a free surface is impossible.

The values of the spall strength of ABS obtained from the analysis of wave profiles in the temperature range of 20–115°C are shown in Fig. 8. It is apparent that an increase of the temperature of the samples to the glass transition temperature results in a gradual decrease of the value of the spall strength. The beginning of glass transition and further heating results in a sharp decrease

of parameters such as density and bulk speed of sound, but the velocity decrement Δu_{fs} increases at the same time. The value of the spall strength does not drop sharply when the glass transition temperature is exceeded, like in case of polycarbonate [12] or PMMA [11], but it decreases only slightly. Moreover, it even slightly increases immediately before the glass transition process in comparison with the spall strength of ABS. This phenomenon can be explained by the influence of competing factors. On the one hand, the mobility of polymer chains should increase during the glass transition, its porosity should increase and its tensile stresses resistance should decrease as a result. On the other hand, an increase of the temperature of the samples results in an increase of the homogeneity of the material shown in [9]. It is quite likely that the heterogeneity of ABS explains the low spall strength at low temperatures. An evaluation of the strain rates in the unloading wave before the spall fracturing showed that a slight increase of the strain rate from $9.3 \cdot 10^4$ to $11.2 \cdot 10^4 \text{ s}^{-1}$ respectively is recorded with an increase of temperatures from 20 to 95°C. The strain rate before the spall fracture decreased at 115°C and amounted to $5 \cdot 10^4 \text{ s}^{-1}$.

Conclusion

Experiments on shock wave loading of ABS samples with an amplitude up to 0.86 GPa in the temperature range 20–115°C with registration of free surface velocity profiles by a VISAR laser interferometer were carried out. The analysis of wave profiles established the dependence of the magnitude of the spall strength on temperature at a maximum compression stress of 0.6 GPa. A slight increase of the value of the spall strength was recorded during the transition from a vitreous state to a highly elastic state, and an explanation of this phenomenon by a change of the internal structure of the material was proposed. The particle velocity and the velocity of the shock wave were measured to calculate the spall strength of ABS in the studied temperature range. Hugoniots of ABS were constructed in the range of maximum shock compression stresses up to 1 GPa in the temperature range 20–115°C based on the experimental data obtained using the known characteristics of soda-lime glass. The bulk speed of sound which is the first term of the linear dependence $U_s = c_0 + bu_p$ decreases with an increase of temperature and the coefficient b slightly changes before reaching the glass transition temperature and sharply decreases when this temperature is exceeded.

Funding

The work was conducted using the equipment of the Moscow Regional Explosion Center of Collective Use, Russian Academy of Sciences, under the state assignment № AAAA-A19-119071190040-5.

Conflict of interest

The authors declare that they have no conflict of interest.

References

- [1] T.J. Holmquist, J. Bradley, A. Dwivedi, D. Casem. *The Europ. Phys. J. Special Topics*, **225**, 343 (2016). DOI: 10.1140/epjst/e2016-02636-5
- [2] N.K. Bourne. *J. Dynamic Behavior Mater.*, **2**, 33 (2016). DOI: 10.1007/s40870-016-0055-5
- [3] J. Richeon, S. Ahzi, K.S. Vecchio, F.C. Jiang, R.R. Adharapurapu. *Intern. J. Solids Structures*, **43**, 7 (2006). DOI: 10.1016/j.ijsolstr.2005.06.040
- [4] L.M. Barker, R.E. Hollenbach. *J. Appl. Phys.*, **41** (10), 4208 (1970). DOI: 10.1063/1.1658439
- [5] B.E. Clements. *AIP Conf. Proceed.*, **1195** (1), 1223 (2009). DOI: 10.1063/1.3295025
- [6] Z.N. Yin, T.J. Wang. *Mater. Sci. Eng.: A*, **527** (6), 1461 (2010). DOI: 10.1016/j.msea.2009.11.025
- [7] A.A. Chevrychkina, G.A. Volkov, A.D. Estifeev. *Proced. Structural Integrity*, **6**, 283 (2017). DOI: 10.1016/j.prostr.2017.11.043
- [8] S. Sharma, S. Chandra, V.M. Chavan, A.K. Nayak. *IOP Conf. Series: Mater. Sci. Eng.*, **1248** (1), 012009 (2022). DOI: 10.1088/1757-899X/1248/1/012009
- [9] S.A. Atroshenko, A.A. Chevrychkina, A.D. Evstifeev, G.A. Volkov. *Phys. Solid State*, **61** (11), 2075 (2019). DOI: 10.1134/S1063783419110052
- [10] E.B. Zaretsky, G.I. Kanel. *J. Appl. Phys.*, **126** (8), 085902 (2019). DOI: 10.1063/1.5116075
- [11] I.A. Cherepanov, A.S. Savinykh, G.V. Garkushin, S.V. Razorenov. *Tech. Phys.*, **68** (5), 622 (2023). DOI: 10.21883/TP.2023.05.56068.10-23
- [12] G.I. Kanel. *TBT*, **58** (4), 596 (2020) (in Russian). DOI: 10.1134/S0018151X20040057
- [13] M.E. Brown, P.K. Gallagher. *Handbook of Thermal Analysis and Calorimetry: Recent Advances, Techniques and Applications* (Elsevier, 2011)
- [14] G.I. Kanel, S.V. Razorenov, A.S. Savinykh, A. Rajendran, Z. Chen. *AIP Conf. Proceed.*, **845**, 876 (2006). DOI: 10.1063/1.2263461
- [15] L.M. Barker, R.E. Hollenbach. *J. Appl. Phys.*, **43** (11), 4669 (1972). DOI: 10.1063/1.1660986
- [16] Yu.B. Kalmykov, G.I. Kanel, I.P. Parkhomenko, A.V. Utkin, V.E. Fortov. *PMTF*, **1**, 126 (1990) (in Russian).
- [17] G.I. Kanel. *Intern. J. Fracture*, **163**, 173 (2010). DOI: 10.1007/s10704-009-9438-0
- [18] G.I. Kanel. *PMTF*, **42** (2), 194 (2001) (in Russian).
- [19] D.O. Kazmer, A.R. Colon, A.M. Peterson, S.K. Kim. *Additive Manufacturing*, **46**, 102106 (2021). DOI: 10.1016/j.addma.2021.102106
- [20] H. Carré, L. Daudeville. *J. Physique IV*, **6** (1), 175 (1996). DOI: 10.1051/jp4:1996117
- [21] J.L. Jordan, D.T. Casem, J. Robinette. *J. Appl. Phys.*, **131** (16), 165903 (2022). DOI: 10.1063/5.0082477
- [22] A.K. Varshneya, J.C. Mauro. *Fundamentals of Inorganic Glasses* (Elsevier, 2019)
- [23] E. Symoens, R. Van Coile, J. Belis. *Glass Structures Eng.*, **7** (3), 457 (2022). DOI: 10.1007/s40940-022-00197-7

Translated by A.Akhtyamov